

ROBUSTNESS AND STABILITY OF POWER-SYSTEM MODELS
USING DAMPING AND SYNCHRONIZING TORQUES

Sherman M. Chan*
Energy Division
Systems Control, Inc.
1801 Page Mill Road
Palo Alto, CA 94304

Michael Athans
Laboratory for Information and Decision Systems
Room 35-308
Massachusetts Institute of Technology
Cambridge, MA 02139

Abstract

The applicability of the recently developed frequency-domain, matrix-norm robustness margins for physical systems is explored in this paper using a power-system example. The power system is modeled using the damping- and synchronizing-torque framework. The robustness margins evaluated at several junctions of the power-system model are shown to be useful measures of the system's tolerance for unmodeled shaft torsional dynamics and variations in the effectiveness of power-system controllers (e.g. multi-terminal high-voltage DC modulators). In addition, the robustness margins are shown to be useful for comparing the robustness of alternate controller designs. This paper ends with general guidelines for applying the matrix-norm robustness margins to physical systems.

I. INTRODUCTION

The newly developed methodology [1-6] for testing the robustness of multi-input, multi-output (MIMO) systems using matrix-norm bounds in the frequency domain represents a true advance in our ability to evaluate the tolerance of a control system to modeling errors. It is widely recognized that such robustness test are conservative in the sense that they are bounds for unstructured perturbations [4]. However, it is not well known that the usefulness of the robustness tests for physical systems can be greatly enhanced by a judicious choice of robustness criteria combine with physical knowledge of specific modeling errors. This paper demonstrates how this can be done in the context of a specific class of problems arising in electric power systems.

This research was supported by the U.S. Department of Energy, Division of Electric Energy Systems, under contract DE-AC01-78RA03395.

* This work was performed while S.M. Chan was with the Laboratory for Information and Decision Systems, Massachusetts Institute of Technology.

The problem is the evaluation of the robustness of a multi-machine power system -- or in power-system parlance, the power system's distance from dynamic instability. The term "dynamic instability" generally refers to spontaneous, growing machine swings in the 0.2-2.0 hz range, but in this paper, the meaning of this term is widened to encompass all spontaneous, unstable oscillations. The sub-synchronous torsional vibrations of generator shafts, for example, is considered here as a form of dynamic instability.

The choice of a frequency-domain power-system model is crucial to the applicability of the robustness theory. The analysis in this paper is carried out using the damping- and synchronizing-torque framework for synchronous machines. A description of this model as well as justifications for its use are given in section III. Some new stability results in terms of damping and synchronizing torques are also presented in this section to facilitate better understanding of this modeling technique.

The remainder of the paper is devoted to the study of power-system robustness. The theorems needed for the analysis are first summarized in section IV, and the application of this theory to the power-system model is illustrated in section V. Finally, we summarize our findings in general terms in the conclusion section (section VI). This information should be of interest to power-system analysts and to other researchers who wish to apply the recently developed robustness theory to physical systems.

II. NOMENCLATURE

I	the identity matrix
$A > 0$	the Hermitian matrix A is positive definite
$A \geq 0$	the Hermitian matrix A is positive semi-definite
$\text{Re}[\bullet]$	the real part of a complex matrix
$\text{Diag}[\bullet]$	a diagonal matrix whose diagonal elements are shown inside the bracket

To be presented at the 20th IEEE Conf. on Decision and Control, San Diego, CA, December 1981.

$\bar{\sigma}(A)$	the maximum singular value of A
$\underline{\sigma}(A)$	the minimum singular value of A
$\ \bullet\ _p$	the matrix norm induced by the vector p -norm. p can be any positive integer or ∞ when it is not specified.

III. MODELING

In choosing a canonical frequency-domain model for a power system, the important criteria are the following.

1. The model must be able to accommodate machine and load models of different complexity.
2. The model must expose junctions at which the uncertainties in the model can be expressed readily in the form of phase and gain variations in each channel of the junction, as well as in cross coupling between the different channels.
3. The perturbed frequency-domain model, or components of the model, must be interpretable in physical terms.

A modeling technique that satisfies these requirements is the damping- and synchronizing-torque framework for synchronous machines.

III.1 Damping and Synchronizing Torques

A synchronous machine can be viewed as a rotating mass driven by the difference between mechanical torques provided by the prime mover and electrical torques originating from electromagnetic interactions between the field and armature circuits. The analytic expression for the electrical torque is generally very complex, as it describes the electric coupling between the machine and the rest of the power system.

A very useful concept in the small-signal analysis of synchronous machines has been the decomposition of the electrical torque into two orthogonal components: a damping component that is in phase with the rotor speed phasor, and a synchronizing component that is in phase with the electrical-angle phasor. The damping and synchronizing torques are so called because in a classical one-machine-versus-infinite-bus system, they are responsible for the damping and the synchronizing restoring forces on the rotor, respectively [7].

The damping- and synchronizing-torque concept can be used to analyze more detailed one-machine-versus-infinite-bus models in which the damping and synchronizing coefficients are no longer constants, but are functions of frequency. It is widely held by practicing engineers that the same physical interpretations for these torques apply at each frequency. In this paper, the damping- and synchronizing-torque concept for n-machine systems is used for studying the stability and robustness of power systems. In the n-machine case, the damping and synchronizing coefficients are frequency-dependent, real-valued, $n \times n$ matrices.

The definition of damping and synchronizing torques for n-machine power systems is based on a linearized model represented in the form shown in figure 1. No assumption regarding the modeling complexity of the network, machine or load is made here (except that all elements in the model must be lumped parameter). The symbols in figure 1 are defined below.

\underline{H}	=	$\text{diag}[2H_1, \dots, 2H_n]$, where H_i is the inertial constant of the i th machine.
$\underline{\omega}(s)$	=	an n -vector containing the changes in shaft speed.
$\underline{T}_e(s)$	=	an n -vector containing the changes in electrical torque.
$\underline{T}_m(s)$	=	an n -vector containing the changes in mechanical torque. It is assumed to be a zero vector in this analysis.
$\underline{T}(s)$	=	a rational, proper, transfer-function matrix which relates the electrical torques to the shaft speeds of the machines.

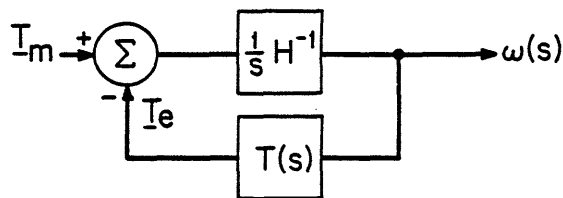


Figure 1: Schematic representation of an n-machine power system.

Definition 1: The damping matrix $\underline{D}(s)$ and the synchronizing matrix $\underline{K}(s)$ are $n \times n$, real-valued matrices such that

$$\underline{D}(s) = \text{Re}[\underline{T}(s)] \quad (1)$$

$$\underline{K}(s) = \text{Re}[s\underline{T}(s)] / \omega_R \quad (2)$$

for all s where $\underline{T}(s)$ is defined. The constant ω_R is the synchronizing speed of the machines.

The damping and synchronizing torques are traditionally defined only for $s=j\omega$. The more general definition here is necessary for studying the stability and robustness properties of synchronous machines. It should be noted that it is not strictly correct to treat damping and synchronizing torques as separate entities, as they are merely different parts of a transfer matrix.

III.2 Stability

For a general one-machine-versus-infinite-bus system (referred to as one-machine system hereafter), the characteristic polynomial is equal to

$$2H s^2 + D(s) s + K(s).$$

When $D(s)$ and $K(s)$ are constants -- as is the case in classical one-machine models, the system is stable if, and only if, both D and K are positive. This stability criterion was extended by deMello and Concordia [8] in a heuristic way to machine models where $D(s)$ and $K(s)$ are functions of frequency. In [8] and in subsequent works (e.g: [9]), the underlying assumptions have been that negative damping torques at the machine-swing frequencies are detrimental to stability, and the addition of positive damping torques at these frequencies always enhances the stability of the machine.

In the following theorem we show in a more precise way that damping and synchronizing torques are sufficient conditions for stability. This theorem, however, does not address the relationship between the damping torques and the time-domain responses.

THEOREM 1: A general one-machine system is asymptotically stable if all the following hold.

- 1) $T(s)$ has no pole in the closed right half-plane.
- 2) $K(0) > 0$
- 3) $D(j\omega) > 0$ for all $\omega > 0$.

A physical interpretation of the conditions of this theorem is as follows. Condition 1 requires that the transfer function $T(s)$ to be stable, which is true in virtually all one-machine systems. Condition 2 is the well-known steady-state stability requirement. It means physically that the rotor must feel a restoring force if it is held at a small distance away from the equilibrium point. Condition 3 requires that the damping torque to be positive at all frequencies. This result can be proved using the Nyquist theorem for single-input, single-output (SISO) systems.

We emphasize that Theorem 1 is a sufficient, but not necessary, condition for stability. In fact, one can easily construct a hypothetical frequency response for which the system is stable, in spite of negative damping torques at some frequencies. Nonetheless, this theorem supports the common assumption that positive damping torques contribute to the stability of a machine. The next theorem shows that a similar result holds for multi-machine power systems.

THEOREM 2: A multi-machine power system is asymptotically stable, except for a pole at the origin, if all of the following hold.

- 1) $T(s)$ has no pole in the closed right half-plane, except for a simple pole at the origin,
- 2) $K(0) + K^T(0) \geq 0$, and the nullity of K is one,
- 3) $D(j\omega) + D^T(-j\omega) - j(K(j\omega) - K^T(-j\omega)) \omega_R/\omega > 0$ for all $\omega > 0$.

The proof of this theorem is given in Appendix A.

It is interesting to note that for a power-system model with classical machines and a purely inductive network, conditions 2 and 3 above simplify to

- 2') $K \geq 0$, and the nullity of K is one, and
- 3') $D > 0$.

A comparison of conditions 2 and 3 of theorem 1 and conditions 2' and 3' of theorem 2 shows that the idea of positive damping and synchronizing torques in one-machine systems has a direct multi-machine extension via the concept of positive definiteness.

Theorem 2 is again a sufficient, but not necessary, condition for stability. For this reason, the damping-and synchronizing-torque framework is not very useful for stability evaluation even for one-machine systems. Other techniques such as eigenvalue analysis in the time domain and Nyquist theorem in the frequency domain are much more effective for checking stability. Nevertheless, the damping- and synchronizing-torque framework is instrumental in providing a physical understanding of the impact of machine controllers on the damping characteristics of synchronous machines. This framework is utilized here in the same spirit for understanding the robustness properties of multi-machine power systems.

IV. ROBUSTNESS THEOREMS

Perturbations of a multiplicative form is considered in this paper because it is found to be the most useful way of applying the robustness theory to the power-system model. Specifically, for a nominal model of the form in figure 2, the actual or perturbed loop transfer matrix $\hat{G}(s)$ is assumed to be related to the nominal loop transfer matrix $\underline{G}(s)$ through the relation

$$\hat{G}(s) = \underline{L}(s) \underline{G}(s) \quad (3)$$

$$\text{or} \quad \hat{G}(s) = \underline{G}(s) \underline{L}(s), \quad (4)$$

where $\underline{L}(s)$ is nominally the identity matrix. The matrix-norm robustness theorems due to Doyle [1] and Lehtomaki [3,5,6] are summarized in the next two theorems.

THEOREM 3: Given a rational, proper transfer matrix $\underline{G}(s)$ of a stable closed-loop system, the closed-loop system with perturbed loop transfer matrix $\hat{G}(s)$, related to $\underline{G}(s)$ through (3) or (4), is closed-loop stable if

- 1) $\underline{G}(s)$ and $\hat{G}(s)$ have the same number of unstable poles and
- 2) $\underline{L}(j\omega)$ has no eigenvalue at 0 or on the negative real axis for all $\omega > 0$, and
- 3) $\| \underline{L}^{-1}(j\omega) - \underline{I} \| < 1 / \| (\underline{I} + \underline{G}(j\omega))^{-1} \|$ for all $\omega > 0$. (5)

THEOREM 4: Given a rational, proper transfer matrix $\underline{G}(s)$ of a stable closed-loop system, the closed-

loop system with a perturbed loop transfer matrix $\hat{G}(s)$, related to $G(s)$ through (3) or (4), is closed-loop stable if

- 1) $G(s)$ and $\hat{G}(s)$ have the same number of unstable poles, and
- 2) $\| \underline{L}(j\omega) - \underline{I} \| < 1 / \| (\underline{I} + \underline{G}^{-1}(j\omega))^{-1} \|$ (6)
for all $\omega > 0$.

It is noteworthy that (5) and (6) become

$$\bar{\sigma}(\underline{L}^{-1}(j\omega) - \underline{I}) < \underline{\sigma}(\underline{I} + \underline{G}(j\omega)) \quad (7)$$

and

$$\bar{\sigma}(\underline{L}(j\omega) - \underline{I}) < \underline{\sigma}(\underline{I} + \underline{G}^{-1}(j\omega)) \quad (8)$$

when the 2 matrix norm is used. Furthermore, it can be shown that when (7) holds as an equality, the "minimum" destabilizing matrix can be written as

$$\underline{L}(j\omega) = (\underline{I} + \sigma_{n-n} \underline{u}_n \underline{v}_n^H)^{-1} \quad (9)$$

where σ_n is the minimum singular value of $\underline{I} + \underline{G}(j\omega)$, and \underline{v}_n and \underline{u}_n are the corresponding singular vectors [5,6]. Similarly, for (8), the "minimum" destabilizing matrix \underline{L} can be written as

$$\underline{L}(j\omega) = \underline{I} + \sigma_{n-n} \underline{u}_n \underline{v}_n^H \quad (10)$$

where σ_n is the minimum singular value of $(\underline{I} + \underline{G}(j\omega))^{-1}$ and \underline{v}_n and \underline{u}_n are the corresponding singular vectors. Lehtomaki [5,6] also showed that when the "projection" of the perturbation on the "worst" direction (9) or (10) is zero, then the "next worst" directions can also be written in terms of singular vectors and singular values. The reader is referred to [5] and [6]. for more details.

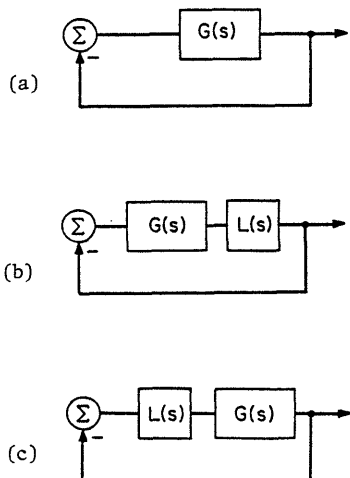


Figure 2: (a) Nominal system. (b) Perturbed system (3). (c) Perturbed system (4).

V. POWER SYSTEM ROBUSTNESS

A schematic representation of a power-system model is shown in figure 3. This diagram is identical to figure 1, except for an additional feedback element $F(s)$ which represents any additional MIMO feedback compensators that are of special interest to the analyst.

The robustness of the closed-loop system is considered with the loop broken at three points labeled 1, 2 and 3 in figure 3. By the term "breaking the loop" we mean that the system model is redrawn as in figure 4a-4c, where the portion enclosed by dotted lines is considered as the nominal loop transfer matrix $\underline{G}(s)$ in each case. The application of the robustness theory to these cases is discussed in turn.

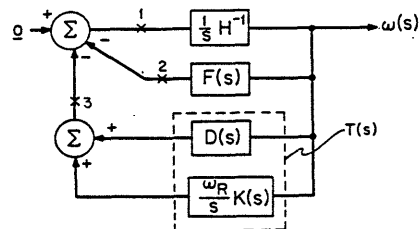


Figure 3: Schematic representation of a power system with a feedback compensator $F(s)$.

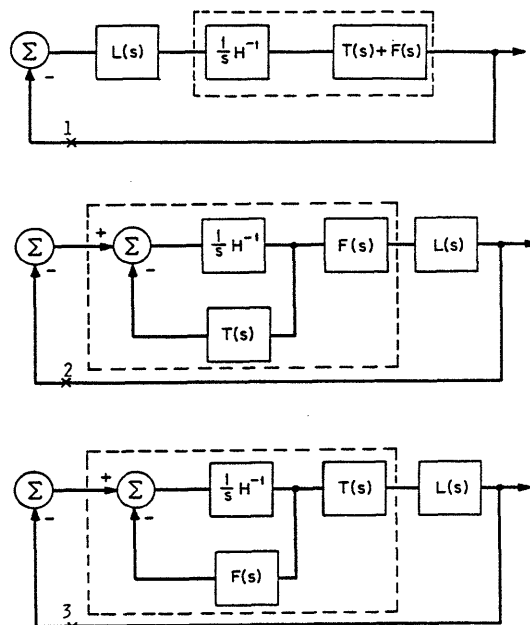


Figure 4: When the loop is broken at points 1, 2 and 3 in figure 3, the system is redrawn to show the loop transfer matrix (enclosed by dotted lines) in each case.

V.1 Robustness at Point 1

The robustness margins at point 1 can be used effectively as a measure of the system's tolerance for unmodeled generator-shaft torsional dynamics.

We assume that the nominal model employs the rigid-shaft model, whose equation of motion is

$$2H \ddot{x}_1(t) = E(t) \quad (11)$$

where x_1 is the angular displacement and E is the torque. The nominal transfer function between $E(s)$ and the speed of the shaft is

$$\frac{sx_1(s)}{E(s)} = \frac{1}{2Hs} \quad (12)$$

The frequency of the first torsional mode of a generator shaft lies in the neighborhood of 10 Hz or higher. Generally only the first mode of oscillation is of importance to the study of torsional vibrations, as the other modes are beyond the bandwidth of most power-system controllers. A detailed model of the shaft capable of modeling the first torsional mode is shown in figure 5. The coefficients k and d are the torsional spring and damping constants, respectively.

The equations of motion of the detailed model are

$$H\ddot{x}_1(t) = k(x_2(t) - x_1(t)) + d(\dot{x}_2(t) - \dot{x}_1(t)) \quad (13)$$

$$H\ddot{x}_2(t) = -k(x_2(t) - x_1(t)) - d(\dot{x}_2(t) - \dot{x}_1(t)) + E(t) \quad (14)$$

It can be shown through straightforward algebraic manipulations that the transfer function between the input torque and output speed is

$$\frac{sx_1(s)}{E(s)} = \frac{1}{2Hs} \frac{ds + k}{\frac{H}{2}s^2 + ds + k} \quad (15)$$

Comparing this equation to the nominal transfer function (12), it is apparent that L in figure 4a is given by

$$L(s) = \frac{ds + k}{\frac{H}{2}s^2 + ds + k} \quad (16)$$

For an n machine system, the matrix $L(s)$ in figure 4a is diagonal, and its elements are given by (16).

The matrices $L-I$ and $L^{-1}-I$ used in the robustness tests (7) and (8) are likewise diagonal, and their elements are given by

$$L(s)-I = \frac{\frac{H}{2}s^2}{\frac{H}{2}s^2 + ds + k} \quad (17)$$

and

$$L^{-1}(s)-I = \frac{\frac{H}{2}s^2}{ds + k} \quad (18)$$

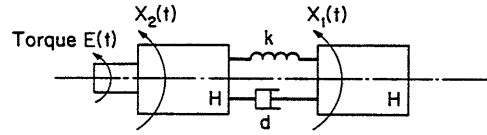


Figure 5: Detailed model of a generator shaft.

The value of $\bar{\sigma}(L-I)$ is easy to compute, since it is simply

$$\max_{i=1,n} |L_i(j\omega) - 1| \quad (19)$$

where L_i-1 is given by (17) for the i th machine.

An analogous result holds for $\bar{\sigma}(L^{-1}-I)$. A direct consequence of (19) is that the perturbations due to two or more shafts with the same resonant frequency are the same as those for just one shaft.

In theory, robustness can be checked using either (7) or (8). But in practice, we find that (7) is not suitable for this type of modeling error because the magnitude of $L^{-1}-I$ increases with frequency, and at the same time, the corresponding robustness margin $\underline{\sigma}(I+G)$ approaches 1 asymptotically at high frequencies. The robustness criterion (8), on the other hand, does not suffer from these shortcomings.

The application of the robustness margin to shaft torsional dynamics is demonstrated below using a 10-machine example where $F(s)$ is a 7-terminal, multiterminal-dc, output-feedback controller [10]. For simplicity, it is assumed that the eigenvalues due to the torsional mode of five of the machines are at $-0.14 \pm j70$, and the other five are at $-0.16 \pm j80$. The per-unit critical damping of these shafts is approximately 0.002, and the natural frequencies are 11 Hz and 13 Hz, respectively. The plots of $\underline{\sigma}(I+G^{-1})$ and $\bar{\sigma}(L-I)$ are shown in figure 6. The curve of $\bar{\sigma}(L-I)$ is seen to be very small at low frequencies and then peaks at the

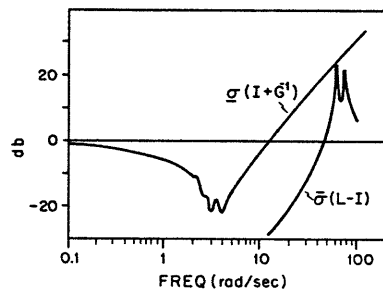


Figure 6: Robustness margins at point 1 and perturbations due to shaft torsional dynamics for a 10-machine, 7-terminal dc/ac power system.

resonant frequencies. The stability of the closed-loop system is guaranteed by (8) for this example, since the magnitude of the perturbations is less than the robustness margin at all frequencies.

V.2 Robustness at Point 2

When designing a feedback controller, the stability margins are usually checked at point 2, or inside $F(s)$, depending on where the physical input channels are located.

Our experience indicates that the robustness margins at the input is most useful for checking tolerances for variations in actuator dynamics. For example, in a multi-terminal dc/ac power system where an exogenous variable (dc voltage) affects the effectiveness of the actuators (dc-current modulators), these margins give ranges of dc-voltage variations for which the system is guaranteed to be closed-loop stable [10]. This application is based on the concept of phase and gain tolerances which are measures of tolerances for multiplicative perturbations that result in a diagonal \underline{L} matrix.

The phase and gain tolerances of MIMO systems can best be explained in terms of the implications of the robustness criteria (7) and (8) for SISO systems. The SISO interpretations apply directly

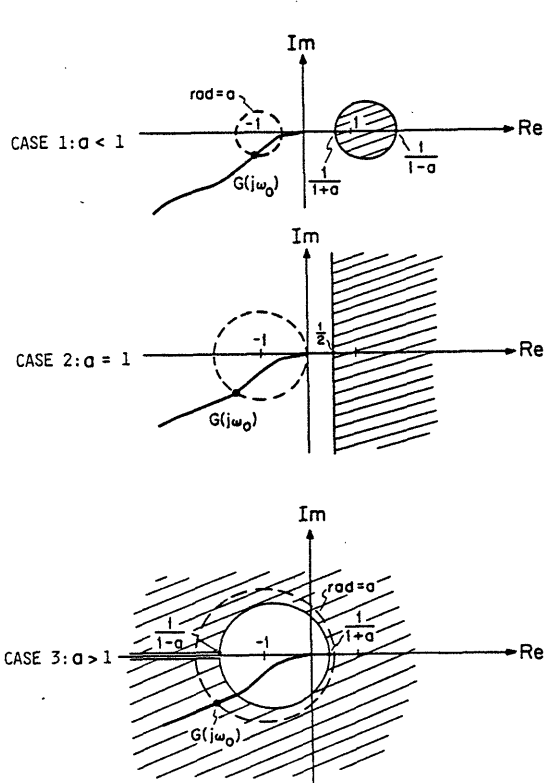


Figure 7: Graphical interpretation of robustness criterion (7).

to the MIMO case because for diagonal \underline{L} matrices (and consequently diagonal $\underline{L}-\underline{I}$ and $\underline{L}^{-1}-\underline{I}$ matrices), criteria (7) and (8) translate simply to magnitude bounds on individual diagonal entries of the $\underline{L}-\underline{I}$ and $\underline{L}^{-1}-\underline{I}$ matrices.

A graphical interpretation is first given for the robustness criterion (7). There are three cases: $a < 1$, $a = 1$ and $a > 1$, where a is the minimum singular value of $\underline{I} + \underline{G}(j\omega)$. In figure 7a, the Nyquist diagram $\underline{G}(j\omega)$ of a hypothetical SISO system is shown on the complex plane. At a fixed frequency ω_0 , a dotted circle with radius a and center at $(-1, 0)$ intersects the Nyquist diagram at $\underline{G}(j\omega_0)$, indicating that $\sigma(\underline{I} + \underline{G}(j\omega_0)) = a$. Equation (7) then implies that $\sigma(\underline{L}^{-1} - \underline{I}) < a$, or equivalently, $\underline{L}(j\omega_0)$ must lie inside a circular, shaded region with center $(1/(1-a^2), 0)$ and radius $a/(1-a^2)$. Similar interpretations apply to the remaining cases in figure 7.

A graphical interpretation of the robustness criterion (8) is given in figure 8. In figure 8a, the dotted circle is the locus of points at which $\sigma(\underline{I} + \underline{G}^{-1}(j\omega_0)) = a$. Thus when the Nyquist diagram intersects this dotted circle at frequency ω_0 , the perturbation $\underline{L}(j\omega_0)$ is constrained to lie within a circular, shaded region in which $\sigma(\underline{L}(j\omega_0) - \underline{I}) < a$.

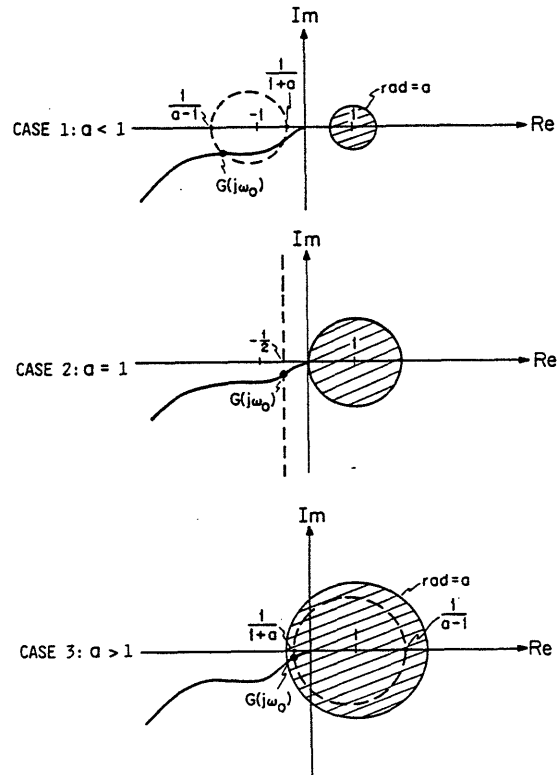


Figure 8: Graphical interpretation of robustness criterion (8).

The gain tolerance at each frequency, based on the robustness criterion (7) (or (8)), is defined as the range of real numbers L for which the perturbed system is guaranteed to be stable. Graphically, the gain tolerance is the part of the real line that lies within the shaded regions in fig. 7 (or figure 8). For example, in case 1 or figure 7, the gain tolerance is the interval $[1/(1+a), 1/(1-a)]$.

The phase tolerance at each frequency, based on the robustness criterion (7) (or (8)), is defined as the largest angle ϕ_0 such that $L = \exp(j\phi)$ satisfies (7) (or (8)) for all $|\phi| < \phi_0$. Again, the phase tolerance can be deduced easily from figure 7 (or figure 8). For example, in case 2 of figure 7, the phase tolerance is 60° .

It is important to emphasize that unlike the familiar concept of phase and gain margins that is defined only at frequencies at which $|G(j\omega)| = 1$, and $\angle G(j\omega) = 180^\circ$, respectively, the phase and gain tolerances are defined at each frequency. The phase and gain tolerances as functions of $\underline{\sigma}(\underline{I} + \underline{G})$ and $\underline{\sigma}(\underline{I} + \underline{G}^{-1})$ are tabulated in tables 1 and 2. For MIMO systems, these bounds represent the maximum allowable simultaneous perturbations for all the channels at the point where the loop is broken.

Table 1: Gain and phase tolerances as a function of the minimum singular value of $\underline{I} + \underline{G}$.

$\underline{\sigma}(\underline{I} + \underline{G})$	gain tolerance	phase tolerance (deg)
0.1	0.9 to 1.1	6
0.3	0.8 to 1.4	17
0.5	0.7 to 2.0	29
0.7	0.6 to 3.3	41
0.9	0.5 to 10.0	53
1.0	0.5 to ∞	60
1.3	0.4 to ∞	81
1.7	0.4 to ∞	107
2.0	0.3 to ∞	120

Table 2: Gain and phase tolerances as a function of the minimum singular value of $\underline{I} + \underline{G}^{-1}$.

$\underline{\sigma}(\underline{I} + \underline{G}^{-1})$	gain tolerance	phase tolerance (deg)
0.1	0.9 to 1.1	6
0.3	0.7 to 1.3	17
0.5	0.5 to 1.5	29
0.7	0.3 to 1.7	41
0.9	0.1 to 1.9	53
1.0	0.0 to 2.0	60
1.3	-0.3 to 2.3	81
1.7	-0.7 to 2.7	116
2.0	-1.0 to 3.0	180

To apply the concept of phase and gain tolerance to the multi-terminal dc/ac power-system example, we observe that the effectiveness of the actuators varies directly with the dc voltage. More precisely, the effects of the variations in dc voltage can be modeled as $\underline{L}(s) = g\underline{I}$, where g is a

non-negative scalar directly related to the change in dc voltage. Since \underline{L} is diagonal and real in this case, the permissible values for g -- and consequently, the range of dc-voltage variations -- can be found directly from the gain-tolerance results in tables 1 and 2 [10].

The robustness margin $\underline{\sigma}(\underline{I} + \underline{G}^{-1})$ at the input can also be used to evaluate the bandwidth of an MIMO system. The reason is that

$$1/\underline{\sigma}(\underline{I} + \underline{G}^{-1}) = \|(\underline{I} + \underline{G})^{-1}\underline{G}\|_2 \quad (20)$$

is equal to the norm of the closed-loop transfer function. Knowing that a matrix norm gives an upper bound on the magnitude of all the matrix elements, it is reasonable to define the maximum MIMO bandwidth as the highest frequency ω at which

$$1/\underline{\sigma}(\underline{I} + \underline{G}^{-1}(j\omega)) = 1. \quad (21)$$

In figure 9 we plotted the function $\underline{\sigma}(\underline{I} + \underline{G}^{-1})$ versus frequency for the dc/ac power-system example. The reader should note the similarity between this curve and the conventional Bode magnitude plot for SISO systems. The MIMO bandwidth is defined as the point where the curve crosses the 0-db line.

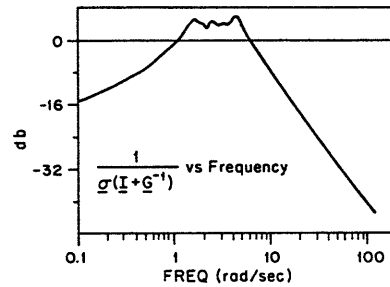


Figure 9: An example demonstrating the evaluation of the maximum MIMO bandwidth.

Finally, it should be pointed out that when $\underline{F}(s)$ is a state-feedback gain found using the linear-quadratic methodology, the inequality

$$\underline{\sigma}(\underline{I} + \underline{G}(j\omega)) > 1 \quad (22)$$

due to Kalman [11] is known to hold at all frequencies (for diagonal control-penalty matrices). Using the results in table 1, we can see that a phase tolerance of 60° and a gain tolerance of $[0.5, \infty)$ always exist at the input [3,5,6,12]. In spite of these seemingly excellent guaranteed phase and gain tolerances, the designer should still give careful considerations to the modeling uncertainties at the input. A neglected high-frequency resonance of an actuator, for example, can introduce a 180° phase shift, which is far in excess of the 60° phase tolerance.

V.3 Robustness at Point 3

An advantage of examining the perturbations at point 3 (of figure 3) is that the destabilizing

multiplicative perturbations can be interpreted directly in terms of the changes in damping and synchronizing torques. Specifically, if $\underline{L}(j\omega)$ is a destabilizing perturbation, then the perturbed damping and synchronizing matrices $\hat{\underline{D}}$ and $\hat{\underline{K}}$ can be computed by

$$\hat{\underline{D}}(j\omega) - \frac{\omega_R}{\omega} \hat{\underline{K}}(j\omega) = \underline{L}(j\omega) [\underline{D}(j\omega) - \frac{\omega_R}{\omega} \underline{K}(j\omega)] . \quad (23)$$

Conversely, if the perturbed matrices $\hat{\underline{D}}$ and $\hat{\underline{K}}$ are known, then \underline{L} can be computed directly from (23).

This application of the robustness theory, unfortunately, is not successful because frequency-domain characterization of possible perturbations in damping and synchronizing matrices is not precisely known at this time.

For a given perturbation in damping and synchronizing matrices, however, we find that the robustness criteria at point 3 are less conservative than those at the input (point 2). At point 2, very small changes in $\underline{D}(s)$ and $\underline{K}(s)$ result in large peaks in $\sigma(\underline{L}-\underline{I})$ and $\sigma(\underline{L}^{-1}-\underline{I})$ near the machine-swing frequencies. This problem is circumvented when the same perturbations are examined at point 3, because the lightly damped, second-order systems consisting of \underline{H}^{-1}/s with "feedback" $\underline{T}(s)$ are disabled by the loop breaking at point 3 (see figure 4). The general conclusion here is that the perturbations in a system element should be examined with the loop broken immediately before or after the element of interest.

The robustness margins at point 3 are found to be useful for comparing the robustness of alternative feedback designs. For example, the robustness margins for three feedback designs for a dc/ac power system are shown in figure 10. It is clear that at frequencies lower than 2 hz, the value of $\sigma(\underline{I}+\underline{G})$ and $\sigma(\underline{I}+\underline{G}^{-1})$ for design 1 are greater than those of the other two designs. Based on this information, it is not correct to conclude that design 1 is the most robust design, since the "smallest" perturbation implicit in the robustness margins for different designs are not the same. However, design 1 is more robust in terms of phase and gain tolerances at low frequencies. In other words, design 1 is more tolerant of variations in the diagonal terms of the damping and synchronizing matrices. We do not yet know if the differences in robustness here are significant in a realistic system. The answer to this question must await more experience on power-system robustness.

VI. CONCLUSION

The application of the recently developed robustness tests for multi-input, multi-output (MIMO) systems is demonstrated in this paper using a power system model. The results indicate that novel modeling techniques coupled with physical understanding of system dynamics are essential to a successful application of the robustness theory. The findings of this paper are summarized in the following.

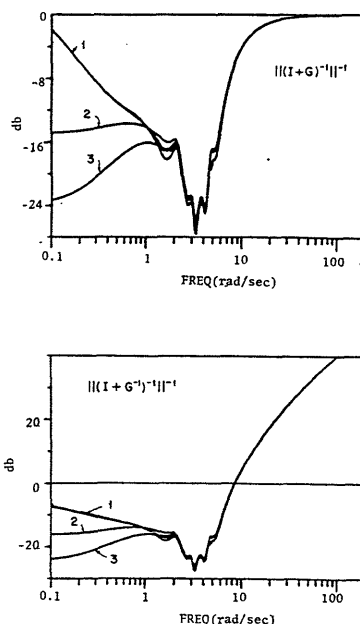


Figure 10: Robustness margins for three alternative feedback designs for a power system.

1. In order to apply the robustness criteria effectively, the system model (in the frequency domain) must expose junctions at which perturbations in each channel, as well as cross couplings between all the channels are physically possible. Moreover, the perturbations at these junctions must be interpretable in physical terms.

2. Perturbations in the multiplicative form appears to be the most useful because perturbations can be interpreted as modeling uncertainties in the physical subsystems rather than as uncertainties in the entire loop transfer matrix. For example, the modeling uncertainties at point 1 of figure 3 are interpreted as perturbations in the transfer function \underline{H}^{-1}/s alone (section V.1).

3. The robustness margins based on the minimum singular value of $\underline{I}+\underline{G}^{-1}$ is found to be extremely useful for checking tolerances for high-frequency modeling errors such as those associated with flexible modes in mechanical structures. The success in this application is due to the ease in characterizing the modeling errors and to the fact that the 180° phase uncertainties associated with this type of modeling errors "closely resembles" the unstructured frequency-domain perturbations for which the robustness criteria are best suited.

4. The robustness margins at the physical inputs can be interpreted as tolerances for modeling errors in the actuators. The concepts of maximum MIMO bandwidth and phase and gain tolerances are introduced to aid physical interpretation of these margins (section V.2). We also emphasize that careful consideration must be given to the uncertainties at the input, even if the guaranteed robustness

margins for linear-quadratic feedback designs are known to exist.

5. In many cases, difficulties are encountered in applying the robustness criteria to modeling uncertainties that are significant at frequencies where the system model is relatively certain. The reason is that the modeling errors in this frequency range are generally highly structured, and they are difficult to characterize in the frequency domain. The recent results in structured perturbations due to Lehtomaki [5,6] is an important advance in this direction. However, we find that Lehtomaki's structures based on the singular-value decomposition of the matrix $\underline{I}+\underline{G}$ or $\underline{I}+\underline{G}^{-1}$ are often incongruous with the modeling errors found in physical systems.

6. The robustness margins may be used for comparing alternate feedback designs for a physical system. Specifically, a design with larger value if $\sigma(\underline{I}+\underline{G})$ or $\sigma(\underline{I}+\underline{G}^{-1})$ is interpreted as more robust in terms of phase and gain tolerances. An example is shown in section V.3 of this paper.

ACKNOWLEDGEMENT

The Fannie and John Hertz Foundation is acknowledged by S.M. Chan for supporting his studies at MIT through a graduate fellowship.

APPENDIX A PROOF OF THEOREM 2

Theorem 2 is proved using the passivity theorem for non-anticipative, linear, time-invariant systems. The passivity theorem in this setting can be stated as follows [13, ch.6]. For a system with plant $\underline{R}(s)$ and feedback compensator $\underline{S}(s)$, the closed-loop system is asymptotically stable if $\underline{R}(s)$ is passive and $\underline{S}(s)$ is strictly passive.

To use the passivity theorem on the power-system model shown in figure 1, the phase-reference pole at the origin must be eliminated; otherwise, both the "plant", \underline{H}^{-1}/s , and the "compensator", $\underline{T}(s)$, are only passive. The transformations

$$\tilde{\underline{H}}^{-1} = \underline{U} \underline{H}^{-1} \underline{U}^{-1} \quad (24)$$

$$\text{and} \quad \tilde{\underline{T}}(s) = \underline{U} \underline{T}(s) \underline{U}^{-1} \quad (25)$$

where

$$\underline{U} = \begin{bmatrix} 1 & 0 & \dots & 0 \\ -1 & 1 & 0 & \dots & 0 \\ -1 & 0 & 1 & 0 & \dots & 0 \\ \vdots & & & & & \vdots \\ -1 & 0 & \dots & 0 & 1 \end{bmatrix} \quad (26)$$

are first applied to make machine 1 the reference machine.

The new plant and compensator models $\hat{\underline{H}}^{-1}/s$ and $\hat{\underline{T}}(s)$ which do not contain the phase-reference pole at the origin are obtained from (24) and (25) by

deleting the first row and column. It can be shown that $\hat{\underline{H}}^{-1}$ is still diagonal and contains the reciprocal of the inertias for machines 2 through n. The plant $\hat{\underline{H}}^{-1}/s$ is therefore passive. Moreover, conditions 1 through 3 of theorem 2 guarantee that the compensator $\hat{\underline{T}}(s)$ is strictly passive. The stability of the closed-loop system follows from the passivity theorem.

REFERENCES

- [1] J.C. Doyle, "Robustness of Multiloop Linear Feedback Systems," Proceedings of the 17th Conf. on Decision and Control, January 1979.
- [2] M.F. Barret, "Conservatism with Sector Based Robustness Tests," Ph.D. dissertation, Univ. of Minnesota, 1980.
- [3] N.A. Lehtomaki, N.R. Sandell, Jr., and M. Athans, "Robustness Results in LQG Based Multivariable Control Designs," IEEE Trans. on Automatic Control, pp.77-92, February 1981.
- [4] J.C. Doyle and G. Stein, "Multivariable Feedback Design: Concept of a Classical/Modern Synthesis," IEEE Trans. on Automatic Control, pp. 4-16, February 1981.
- [5] N.A. Lehtomaki, "Practical Robustness Measures in Multivariable Control Systems Analysis," Ph.D. dissertation, Massachusetts Institute of Technology, 1981.
- [6] N.A. Lehtomaki, B. Levy, et al., "Robustness Tests Utilizing Structure of Modeling Errors," to be presented at the 21st Conf. on Decision and Control, December 1981.
- [7] P.M. Anderson and A.A. Fouad, Power System Control and Stability, Ames, IA: Iowa State Univ. Press, 1976.
- [8] F.P. deMello and C. Concordia, "Concept of Synchronous Machine Stability Affected by Excitation Control," IEEE Trans. on Power Apparatus and Systems, pp. 316-329, April 1969.
- [9] M. Mobarak, D. Thorne and E. Hill, "Contrast of Power System Stabilizer Performance on Hydro and Thermal Units," IEEE Trans. on Power Apparatus and Systems, pp.1522-1533, July 1980.
- [10] S.M. Chan, "Small Signal Control of Multiterminal DC/AC Power Systems," Ph.D. dissertation, Massachusetts Institute of Technology, 1981.
- [11] R. Kalman, "When is a Linear System Optimal?" Trans. ASME Ser. D:Journal of Basic Engineering, pp. 51-60, 1964.
- [12] M.G. Safonov and M. Athans, "Gain and Phase Margins of Multiloop LQG Regulators," IEEE Trans. on Automatic Control, pp. 173-178, April 1977.
- [13] C.A. Desoer and M. Vidyassagar, Feedback Systems: Input-Output Properties, New York, NY: Academic Press, 1975.